

# GPR40-Mediated $G\alpha_{12}$ Activation by Allosteric Full Agonists Highly Efficacious at Potentiating Glucose-Stimulated Insulin Secretion in Human Islets<sup>§</sup>

Marie-Laure Rives, Brian Rady, Nadia Swanson, Shuyuan Zhao, Jenson Qi, Eric Arnoult, Ivona Bakaj, Arturo Mancini, Billy Breton, S. Paul Lee, Mark R. Player, and Alessandro Pocai

*Molecular and Cellular Pharmacology, Janssen Research & Development, LLC, La Jolla, California (M.-L.R., N.S.); Cardiovascular and Metabolism (B.R., S.Z., J.Q., I.B., S.P.L., M.R.P., A.P.), and Computational Chemistry (E.A.), Janssen Research & Development, LLC, Spring House, Pennsylvania; and Domain Therapeutics NA Inc., Montreal, Quebec, Canada (A.M., B.B.)*

Received December 7, 2017; accepted March 20, 2018

## ABSTRACT

GPR40 is a clinically validated molecular target for the treatment of diabetes. Many GPR40 agonists have been identified to date, with the partial agonist fasiglifam (TAK-875) reaching phase III clinical trials before its development was terminated due to off-target liver toxicity. Since then, attention has shifted toward the development of full agonists that exhibit superior efficacy in preclinical models. Full agonists bind to a distinct binding site, suggesting conformational plasticity and a potential for biased agonism. Indeed, it has been suggested that alternative pharmacology may be required for meaningful efficacy. In this study, we described the discovery and characterization of Compound A, a newly identified GPR40 allosteric full agonist highly efficacious in human islets at potentiating glucose-stimulated insulin secretion.

We compared Compound A-induced GPR40 activity to that induced by both fasiglifam and AM-1638, another allosteric full agonist previously reported to be highly efficacious in preclinical models, at a panel of G proteins. Compound A was a full agonist at both the  $G\alpha_q$  and  $G\alpha_{i2}$  pathways, and in contrast to fasiglifam Compound A also induced  $G\alpha_{12}$  coupling. Compound A and AM-1638 displayed similar activity at all pathways tested. The  $G\alpha_{12}/G\alpha_{13}$ -mediated signaling pathway has been linked to protein kinase D activation as well as actin remodeling, well known to contribute to the release of insulin vesicles. Our data suggest that the pharmacology of GPR40 is complex and that  $G\alpha_{12}/G\alpha_{13}$ -mediated signaling, which may contribute to GPR40 agonists therapeutic efficacy, is a specific property of GPR40 allosteric full agonists.

## Introduction

Activation of the free fatty acid receptor 1, also known as GPR40, potentiates glucose-stimulated insulin secretion (GSIS) from pancreatic  $\beta$ -cells and stimulates the release of incretins, such as glucagon-like peptide 1 (GLP-1), from enteroendocrine cells (Briscoe et al., 2003, 2006; Itoh et al., 2003; Yonezawa et al., 2004; Hardy et al., 2005; Shapiro et al., 2005; Tomita et al., 2005; Latour et al., 2007; Edfalk et al., 2008; Stoddart et al., 2008; Luo et al., 2012; Mancini and Poitout, 2013). GLP-1 further promotes GSIS and also decreases hepatic gluconeogenesis, inhibits glucagon secretion,

reduces body weight, and improves insulin sensitivity (Baggio and Drucker, 2007; Holst, 2007; Pocai, 2012; Gorski et al., 2017). Thus, the dual mechanisms of GPR40 in pancreatic  $\beta$ -cells as well as in enteroendocrine cells provide considerable rationale for the development of GPR40 agonists for the treatment of type-2 diabetes mellitus (T2DM), with a potential for weight management.

A number of potent, synthetic GPR40 agonists have been reported and a GPR40 partial agonist, fasiglifam from Takeda, advanced as far as phase III clinical trials (Kaku et al., 2015). In a phase II study in T2DM patients, fasiglifam induced a similar glucose-lowering effect (HbA1c: ca. 1%) to that of glimepiride (Burant et al., 2012; Leifke et al., 2012). In spite of similar promising results in phase III, fasiglifam was withdrawn from development due to drug-induced liver injury (Hedrington and Davis, 2014; Otieno et al., 2017).

Since then, numerous full agonists with superior efficacy both in vitro and in vivo compared with fasiglifam have been

This research was supported by Janssen, Pharmaceutical Companies of Johnson & Johnson.

The authors declare no conflict of interest.

<https://doi.org/10.1124/mol.117.111369>.

§ This article has supplemental material available at [molpharm.aspetjournals.org](http://molpharm.aspetjournals.org).

**ABBREVIATIONS:** AgoPAM, allosteric agonist with PAM activity; BRET, bioluminescence resonance energy transfer; BSA, bovine serum albumin; CHO, Chinese hamster ovary; CPM, counts per minute; DMEM, Dulbecco's modified Eagle's medium; FBS, fetal bovine serum; GLP-1, glucagon-like peptide 1; GPR40, free fatty acid receptor 1, also known as GPR40; GSIS, glucose-stimulated insulin secretion; HbA1c, haemoglobin A1c; HBSS, Hanks' balanced salt solution; HTRF, homogeneous time-resolved fluorescence; IBMX, 3-isobutyl-1-methylxanthine; IP1, inositol-1-phosphate; PAM, positive allosteric modulator; PBS, phosphate-buffered saline; PEI, polyethylenimine; PKD, protein kinase D; PTX, pertussis toxin; T2DM, type-2 diabetes mellitus.

reported (Defossa and Wagner, 2014; Li et al., 2016). Interestingly, these full agonists bind to a recently identified binding site, distinct from previously predicted pockets, and different from that of endogenous fatty acids and fasiglifam or other partial agonists (Lin et al., 2012; Defossa and Wagner, 2014; Hauge et al., 2014; Srivastava et al., 2014; Lu et al., 2017). The presence of multiple binding sites suggests conformational plasticity, highlighting a potential for biased agonism (Kenakin et al., 2012; Kenakin and Christopoulos, 2013; Costa-Neto et al., 2016; Rankovic et al., 2016). GPR40 is mostly known to couple to the heterotrimeric G protein  $G_{\alpha q/11}$  (Shapiro et al., 2005). However, it has also been shown that GPR40 could couple to other pathways in a ligand-dependent manner and that only allosteric full agonists able to induce the activation of such alternative pathways, such as the  $G_{\alpha s}$ /cAMP pathway, could trigger maximal efficacy in pre-clinical models (Lin et al., 2012; Defossa and Wagner, 2014; Hauge et al., 2014). GPR40 has also been shown to couple to  $G_{\alpha i/o}$  and arrestin (Schröder et al., 2011; Mancini et al., 2015), and arrestin recruitment has been shown to contribute to GPR40-mediated GSIS (Mancini et al., 2015).

Through a rational design approach, we have identified a new human GPR40 (hGPR40) full agonist at the  $G_{\alpha q}$ /inositol-1-phosphate (IP1)/calcium pathway fully efficacious at enhancing GSIS in human islets. We compared Compound A-induced GPR40 activity at a panel of G proteins and to that induced by both fasiglifam as well as AM-1638, previously reported as a highly efficacious hGPR40 allosteric full agonist (Hauge et al., 2014; Li et al., 2016). Our data indicated that Compound A and AM-1638 were both hGPR40 allosteric full agonists, not only at the  $G_{\alpha q}$  pathway but also at  $G_{\alpha i2}$ , with no to very weak efficacy at the  $G_{\alpha s}$ /cAMP pathway. Interestingly, in contrast to fasiglifam and  $\alpha$ -linolenic acid, Compound A and AM-1638 strongly engaged the  $G_{\alpha 12}$  protein. Our data suggest that the pharmacology of GPR40 is complex and that  $G_{\alpha 12}$ / $G_{\alpha 13}$ -mediated signaling, which may contribute to the release of vesicles possibly via protein kinase D (PKD) activation and actin remodeling, is a specific property of the GPR40 allosteric full agonists Compound A and AM-1638.

## Materials and Methods

**Cell Lines and Cell Culture.** The hGPR40 low-expressing stable Chinese hamster ovary (CHO)-K1 cell line used in this study was purchased from Multispan, Inc (Hayward, CA). The receptor density in this cell line was evaluated by whole cell radioligand saturation binding at  $47,112 \pm 5,088$  receptors per cell, which was comparable to the GPR40 density in a rat insulinoma  $\beta$ -cell line INS-1 832/13 ( $41,519 \pm 9,516$  receptors per cell). Cells were maintained in Dulbecco's modified Eagle's medium (DMEM)/F-12 supplemented with 10% fetal bovine serum (FBS), 1% penicillin/streptomycin, and 10  $\mu$ g/ml puromycin, and then incubated at 37°C with 5% CO<sub>2</sub>.

**IP1 Homogeneous Time-Resolved Fluorescence (HTRF) Assay.** The day before the assay, hGPR40-expressing CHO-K1 cells were plated overnight in 384-well plates (4,000 cells per well) in complete media, with or without 100 ng/ml pertussis toxin (PTX) (Tocris Bioscience, Bristol, United Kingdom). The following day, the culture medium was replaced with assay buffer containing Hanks' balanced salt solution (HBSS) with calcium and magnesium, 20 mM HEPES, and 0.1% fatty acid free bovine serum albumin (BSA), pH 7.4. Compounds were then added and incubated with cells at 37°C for 90 minutes. Analytes were detected according to the manufacturer's protocol (IPone Tb kit; CisBio, Codolet, France). Data presented are representative of at least three independent experiments

performed in quadruplicate for each compound. Data are represented as averages  $\pm$  S.D.

**Calcium Measurements.** The day before the assay, hGPR40-expressing CHO-K1 cells were plated overnight in 384-well plates (20,000 cells per well) in complete media. The following day, the culture medium was replaced with 25  $\mu$ l of assay buffer containing HBSS with calcium and magnesium, 20 mM HEPES, and 0.1% fatty acid free BSA, pH 7.4, and then starved for 1 hour at 37°C. Calcium-sensitive fluorescent dye (Fluo 6; Molecular Devices, San Jose, CA) was then added in 25  $\mu$ l assay buffer and the cells were incubated for another hour at 37°C and protected from light. Plates were read on FLIPR Tetra (Molecular Devices) measuring emission at 515–575 nm caused by excitation at 470–495 nm before and up to 8 minutes after addition of 12.5  $\mu$ l of 5X agonist solution (prepared in assay buffer). The concentration response curves were constructed based on the maximal responses over baseline obtained for different concentrations of each compound. Data presented are representative of three independent experiments performed in quadruplicate for each compound. Data are represented as averages  $\pm$  S.E.M.

**cAMP HTRF Measurements.** The day before the assay, hGPR40-expressing CHO-K1 cells were plated overnight in 384-well plates (20,000 cells per well) in complete media. The following day, the culture medium was replaced with assay buffer containing HBSS with calcium and magnesium, 20 mM HEPES, and 0.1% fatty acid free BSA, pH 7.4, and then starved for 1 hour at 37°C. The assay buffer was then replaced with fresh assay buffer containing 500  $\mu$ M IBMX, and compounds were added in assay buffer (no IBMX) for 30 minutes. Analytes were detected according to the manufacturer's protocol (cAMP Dynamic kit; CisBio). Fluorescence was read with a PHERAstar plate reader (BMG Labtech, Ortenberg, Germany) using an excitation of 337 nm and emissions of 620 and 665 nm. Raw data were converted to nanomolar cAMP values by interpolation from a cAMP standard curve. The maximum effect attributable to the drug ( $E_{max}$ ) and EC<sub>50</sub> determinations were made from an agonist-response curve analyzed with a curve fitting program using a four-parameter logistic dose-response equation in GraphPad Prism 7.0 (GraphPad Software, Inc., La Jolla, CA). Data presented are representative of three independent experiments performed in quadruplicate for each compound. Data are represented as averages  $\pm$  S.D.

**DiscoverX Arrestin Recruitment.** The ability of hGPR40 to recruit  $\beta$ -arrestin-2 was determined using the DiscoverX PathHunter technology (DiscoverX, Fremont, CA) that involves enzyme complementation of a fusion-tagged receptor along with an arrestin recruitment modulating sequence and  $\beta$ -arrestin-2 proteins. DLD1 cells expressing hGPR40 (DiscoverX) were seeded in Cell Plating Media 2 (DiscoverX) at a density of 15,000 cells/well in 384-well black, clear-bottom plates. The following day, the culture medium was replaced with assay buffer containing HBSS with calcium and magnesium, 20 mM HEPES, and 0.1% fatty acid free BSA, pH 7.4, and then starved for 1 hour at 37°C. The cells were then treated with multiple concentrations of agonists in phosphate-buffered saline (PBS) and incubated at 37°C for 60 minutes. DiscoverX reagent was then added to the cells according to the manufacturer's recommendations, followed by 1 hour incubation at room temperature, and then luminescence was measured on the PHERAstar reader. Data presented are representative of three independent experiments performed in triplicate for each compound. Data are represented as averages  $\pm$  S.D.

**Bioluminescence Resonance Energy Transfer (BRET)-Based Biosensor Assays (BioSensAll).** BioSensAll biosensor assays were conducted at Domain Therapeutics NA Inc. (Montreal, QC, Canada). Assays were performed in HEK-293T cells, cultured in DMEM (Wisent, Quebec, Canada) supplemented with 1% penicillin-streptomycin (Wisent, Quebec, Canada) and 10% FBS (Wisent, Quebec, Canada), and then maintained at 37°C with 5% CO<sub>2</sub>. All biosensor-coding plasmids and related information are the property of Domain Therapeutics NA Inc.: GAPL-Gs, GAPL-Gq, GAPL-G11, GAPL-Gi2, GAPL-GoB, GAPL-Gz, and GAPL-G12. Transfections were performed

using 25-kDa linear polyethylenimine (PEI) (Polysciences, Warrington, PA) at a 3:1  $\mu\text{l}$  of PEI/microgram of DNA ratio. Briefly, DNA and PEI were diluted separately in 150 mM NaCl, mixed, and then incubated for at least 20 minutes at room temperature [note: the total amount of DNA transfected was adjusted to a final quantity of 2  $\mu\text{g}$  with salmon sperm DNA (Thermo Fisher Scientific, Waltham, MA)]. During the 20-minute incubation, HEK-293T cells were detached, counted, and resuspended into cell culture medium to a final density of 350,000 cells/ml. At the end of the 20-minute incubation, DNA/PEI complexes were added to the cells followed by gentle mixing. Cells were subsequently distributed in cell culture-treated 96-well plates (White Opaque 96-well Microplates; Greiner Kremsmünster, Austria) at a density of 35,000 cells per well (i.e., 100  $\mu\text{l}$  of cell suspension per well) and incubated at 37°C for 48 hours. For PTX treatment, 24 hours after transfection and the day before the assay the medium was replaced by fresh medium containing 100 ng/ml PTX (Tocris Bioscience). Then, 48 hours after transfection, the transfection medium was removed and cells were washed once with 100  $\mu\text{l}$  of Tyrode-HEPES buffer (Sigma-Aldrich, St. Louis, MO) per well. Wash buffer was then replaced with 100  $\mu\text{l}$  of fresh Tyrode-HEPES buffer per well and plates were incubated for 60 minutes at room temperature. At the end of this equilibration period, 10  $\mu\text{l}$  of 20  $\mu\text{M}$  e-Coelenterazine ProLume Purple (Methoxy e-CtZ; Nanolight, Pinetop, AZ) was added to each well followed immediately by the addition of increasing test compound concentrations. For PAM mode experiments, 10 minutes after the addition of increasing concentrations of test compound, an EC<sub>20</sub> of  $\alpha$ -linolenic acid (1  $\mu\text{M}$ ) was added to the cells. Cells were incubated at room temperature for 10 minutes and BRET readings were subsequently collected with a 0.4-second integration time on a Synergy NEO plate reader (BioTek Instruments, Inc., Winooski, VT; filters: 400/70 and 515/20 nm, donor and acceptor filters, respectively). The BRET signal was calculated as the ratio of acceptor emission to donor emission. Data from at least three independent experiments for each compound and performed in duplicates were combined and the symbols presented are the mean  $\pm$  S.E.M. Note that due to the nature of the sensors, apart from the GAPL-Gs sensor, whose activation leads to a decrease in the BRET signal, activation of the other sensors leads to an increase in the BRET signal.

To calculate the bias factor between some of those pathways for our compounds, we used the Black-Leff operational model to fit the agonist concentration ([A])-response curves as follows (Kenakin et al., 2012):

$$\text{Response} = \frac{E_m [A]^n \tau^n}{[A]^n \tau^n + ([A] + K_A)^n}$$

where the maximal response of the system is given by  $E_m$ ;  $n$  is the transducer slope for the function linking agonist concentration to measured response; and parameters  $K_A$  and  $\tau$  are the equilibrium constants governing the reaction.  $\log(\tau/K_A)$  is defined as the transduction coefficient, and using  $\alpha$ -linolenic acid as a reference we calculated the relative efficiency of our compounds at relevant pathways [ $\Delta\log(\tau/K_A)$ ]. The bias factor [ $\Delta\Delta\log(\tau/K_A)$  or log bias] between pathways  $j_1$  and  $j_2$  can be calculated as follows:

$$\text{Bias} = 10^{\Delta\Delta\log(\tau/K_A)_{j_1-j_2}}$$

where

$$\Delta\Delta\log(\tau/K_A)_{j_1-j_2} = \log \text{bias} = \Delta\log(\tau/K_A)_{j_1} - \Delta\log(\tau/K_A)_{j_2}$$

**Molecular Modeling.** Molecular modeling and docking have been performed using the recent co-crystal structure of hGPR40 in complex with MK-8666 and AgoPAM AP8 (PDB code 5TZY) (Lu et al., 2017). Molecular Operating Environment 2015.1001 (Chemical Computing Group Inc., Montreal, QC, Canada) was used for loop modeling, energy minimization (AMBER10:EHT forcefield and Born solvation model), and rescoring of the docking poses. Glide was used for molecular docking of Compound A (Small-Molecule Drug Discovery Suite 2016-3: Glide, version 6.9; Schrödinger, LLC New York, NY). The

docking poses generated with Glide-XP were rescored using the GBVI/WSA dG scoring function available in Molecular Operating Environment 2015.1001 (Corbeil et al., 2012). The top ranked pose of Compound A was imported, with the hGPR40 protein structure, into a Pymol session to create all of the pictures (The PyMOL Molecular Graphics System, version 1.8; Schrödinger, LLC).

**Radioligand Binding Experiment.** Membranes were prepared as follows. Cells stably expressing hGPR40 were harvested by centrifugation (10 minutes at 5,000g). The pellet was resuspended in lysis buffer [10 mM Tris-HCl, pH 7.4, 137 mM NaCl, and complete protease inhibitor cocktail (1 tablet per 40 ml; Roche, Basel, Switzerland)], and lysed using 30 strokes with a dounce homogenizer on ice. The homogenate was centrifuged at 4°C (10 minutes at 900g). The supernatant was centrifuged at 4°C for 60 minutes at 100,000g. The resulting pellet was resuspended in wash buffer [10 mM Tris-HCl, pH 7.4, 1 M NaCl, and complete protease inhibitor cocktail (1 tablet per 40 ml)]. The homogenate was centrifuged at 4°C for 30 minutes at 100,000g. Membranes were resuspended at 10 mg/ml protein in 10 mM Tris-HCl, pH 7.4, and 137 mM NaCl.

Test compounds were serially diluted in binding buffer (PBS + 0.1% fatty acid-free BSA). Each well of the 96-well assay plate contained diluted test compounds, 50 nM [<sup>3</sup>H]-Compound A or 10 nM [<sup>3</sup>H]-AM-1638, and 10  $\mu\text{g}$ /well hGPR40 membrane suspension in a total volume of 100  $\mu\text{l}$ . The binding reaction was allowed to equilibrate for 60 minutes at room temperature with shaking. Binding assays were terminated using a Harvester Filtermate 96 (PerkinElmer, Waltham, MA). Bound and free radioligands were separated by collecting the membrane-bound fraction onto GF/B filter plates impregnated with PEI 0.5% and prewetted with binding buffer. Filter plates were washed four times with ice-cold binding buffer and dried for 2 hours. Microscint O (50  $\mu\text{l}$ ) was added to each well and radioactivity was counted using Topcount (PerkinElmer). Nonspecific binding was determined using 10  $\mu\text{M}$  cold Compound A or AM-1638. Data analysis was performed using GraphPad Prism 7.0 (GraphPad Software, Inc.). Data presented are representative of three independent experiments performed in triplicate for each compound. Data are represented as averages  $\pm$  S.D.

For receptor densities evaluation, whole cell saturation binding experiments were performed according to what has been previously described (Jin et al., 2009), using a binding buffer composed of DMEM, 25 mM HEPES, and 0.1% fatty acid-free BSA (pH 7.4). For receptor number determination, a normalization sample (NORM) was used and the receptor density was calculated as follows:

$$\begin{aligned} \text{Number of receptors per cell} \\ = \frac{6.022 \times 10^{23} \times B_{\text{max}} \times \text{number of mol radioligand used for NORM}}{\text{Number of cells} \times \text{CPM of NORM}} \end{aligned}$$

**Insulin Secretion in Human Islets.** Human islets were dispersed with Accutase (Thermo Fisher Scientific, Waltham, MA) for 10 minutes at 37°C. Twenty thousand cells per well were plated in V-bottom 96-well plates and cultured overnight in complete medium containing: CMRL Media (Thermo Fisher Scientific), 10 mM Niacinamide, (1 mg/ml, 0.55 mg/ml, 0.67  $\mu\text{g}$ /ml insulin-transferrin-selenium) ITS (Thermo Fisher Scientific), 16.7 mM zinc sulfate, 5 mM sodium pyruvate, 2 mM glutamax (Thermo Fisher Scientific), 25 mM HEPES, and 10% FBS. The next day, medium was replaced with assay buffer (Krebs Ringer) and cells were preincubated in 2 mM glucose for 1 hour. Next, the indicated concentrations of compounds were added in either 2 or 12 mM glucose and the cells were incubated at 37°C for 1 hour. The supernatant was then collected and tested for insulin using the CisBio HTRF insulin assay kit. Data are represented as averages  $\pm$  S.E.M. from three different islets. Donors are different between Figures 2A and 2B. Statistical significance was determined by one-way analysis of variance with Dunnett's post hoc analysis using GraphPad Prism 7.0 (GraphPad Software, Inc.).

**Statistics.** All data are expressed as the mean  $\pm$  S.E.M. or S.D. as indicated in *Materials and Methods* and the figure legends of the

indicated number of experiments. Statistical significance was determined by one-way analysis of variance (ANOVA) with Dunnett's post hoc analysis using GraphPad Prism 7.0 (GraphPad Software, Inc.).

**Materials.** The synthesis of Compound A is summarized in the Supplemental Methods. Forskolin and IBMX were obtained from Tocris Bioscience. DMEM/F12 and DMEM/high glucose media, penicillin/streptomycin, L-glutamine, G418, and hygromycin were purchased from Thermo Fisher Scientific. FBS was purchased from Hyclone, GE Healthcare Life Sciences (Logan, UT). HBSS and HEPES were purchased from CellGro, Corning Inc. (Corning, NY). Fatty acid free BSA was purchased from Sigma-Aldrich (St. Louis, MO). Human islets were obtained from healthy donors through Prodo Laboratories Inc. (Aliso Viejo, CA).

## Results

### Identification and Characterization of a New hGPR40 Full Agonist

**Compound A Is a Full Agonist at the IP1/Calcium Pathway.** Multiple series of hGPR40 agonists were rationally designed based on existing structures and evaluated in a calcium assay using a hGPR40 low-expressing CHO-K1 stable cell line to allow differentiation between partial and full agonists. In this assay, Compound A (Fig. 1A; Supplemental Methods) showed similar efficacy to AM-1638, previously reported as a highly efficacious hGPR40 full agonist (Hauge et al., 2014; Li et al., 2016), while fasiglifam was only weakly efficacious (Fig. 1B). To confirm the activity of Compound A, we used an IP1 HTRF assay, which detects the accumulation of IP1 inside the cells that follows the rapid degradation of IP3 (Fig. 1C). The IP1 HTRF assay has indeed been shown to generate less false positive results (Cassutt et al., 2007). Compound A was as efficacious as AM-1638 and showed superior efficacy compared with fasiglifam ( $E_{\max}$  fasiglifam =  $50.9\% \pm 1.2\%$  compared to that of Compound A; \*\*\*\* $P < 0.0001$ ) (Fig. 1C). However, compared to Compound A and AM-1638 ( $EC_{50} = 225 \pm 80$  and  $158 \pm 27$  nM, respectively) (Fig. 1C), fasiglifam ( $EC_{50} = 78 \pm 30$  nM) was about two to three times more potent (\* $P < 0.05$ ).

We also profiled the activity of Compound A at the  $\beta$ -arrestin2 pathway and obtained similar results (Supplemental Fig. 1), with fasiglifam inducing about 50% efficacy compared with the full agonists ( $51.2\% \pm 8.3\%$ ; \*\*\*\* $P < 0.0001$ ). No significant bias was observed for any of the compounds between  $G_{\alpha q/11}$  and  $\beta$ -arrestin2.

### Compound A Is Fully Efficacious at Potentiating GSIS in Human Islets.

We then tested the ability of Compound A to potentiate GSIS in human islets from healthy donors. All donors tested were responsive to 12 mM glucose and non glucose-dependent insulin secretagogues, KCl, and glibenclamide. In the presence of 12 mM glucose, Compound A (3 and 10  $\mu$ M) significantly potentiated insulin secretion ( $79.6 \pm 18.5$  and  $78.7 \pm 10.2$  ng/ml, respectively;  $P < 0.0001$ ) compared with islets treated with glucose alone ( $11.6 \pm 6.2$  ng/ml) (Fig. 2A). Fasiglifam potentiated 12 mM glucose-induced insulin secretion ( $26.7 \pm 15.9$  ng/ml;  $P = 0.0008$ ) but to a lesser extent than Compound A ( $22.4\% \pm 6\%$  of the potentiation induced by Compound A;  $P < 0.0001$ ). The effects observed with Compound A and fasiglifam were consistent with the potentiation induced by AM-1638 compared with other partial agonists (Luo et al., 2012). Interestingly, in the presence of 2 mM glucose fasiglifam was inactive, whereas Compound A (3 and 10  $\mu$ M) significantly potentiated insulin secretion ( $16.6 \pm 4.7$  and  $41.2 \pm 12.1$  ng/ml, respectively;  $P < 0.0001$ ) compared with islets treated with glucose alone ( $3.9 \pm 1.2$  ng/ml) (Fig. 2B).

### Compound A Is an Allosteric Full Agonist at $G_{\alpha q}$ , $G_{\alpha i2}$ , and $G_{\alpha 12}$

#### Compound A Is a Full Agonist at $G_{\alpha q}$ and $G_{\alpha i2}$ , and Engages the $G_{\alpha 12}$ Pathway.

In addition to the  $G_{\alpha q}$ /IP1/calcium pathway, some GPR40 agonists have been shown to activate alternative pathways (Schröder et al., 2011; Lin et al., 2012; Defossa and Wagner, 2014; Hauge et al., 2014; Mancini et al., 2015). Thus, we used BRET-based biosensors to fully characterize other G proteins downstream from hGPR40 activation. Resonance energy transfer between a luminescent enzymatic donor and a fluorescent protein acceptor typically occurs in the 1–10 nm range, which makes BRET an ideal platform to study protein-protein interactions in living cells. BRET has indeed been extensively used to study G protein activation by multiple GPCRs (Denis et al., 2012; Salahpour et al., 2012; Namkung et al., 2016) and allows monitoring in real time the activation of G proteins of interest following GPR40 agonist treatment. We first used  $G_{\alpha q}$  and  $G_{\alpha 11}$  sensors (Fig. 3A; Supplemental Fig. 2A) to confirm the engagement of those pathways. IP1 production can indeed originate from other G protein couplings (Rives et al., 2009)

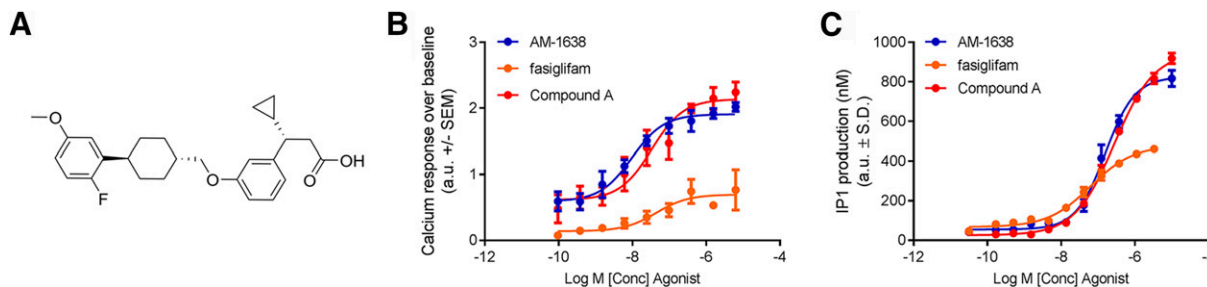


**Fig. 1.** Identification of a new full hGPR40 agonist, Compound A, at the  $G_{\alpha q}$ /IP1/calcium pathway. (A) Structure of Compound A. (B) Calcium signaling in a CHO-K1 cell line stably expressing hGPR40. Compound A showed similar efficacy to AM-1638, previously reported as a highly efficacious hGPR40 full agonist and fasiglifam was only partially efficacious. Data presented are representative of three independent experiments performed in quadruplicate for each compound. Data are represented as averages  $\pm$  S.E.M. (C) In a CHO-K1 cell line stably expressing hGPR40, Compound A was a full agonist at the IP1 pathway, with similar efficacy as AM-1638. Fasiglifam was a partial agonist with about 50% efficacy ( $50.9\% \pm 1.2\%$ ;  $P < 0.0001$ ) compared with Compound A and AM-1638. Data presented are representative of three independent experiments performed in quadruplicate for each compound. Data are represented as averages  $\pm$  S.D. Statistical significance was determined by one-way ANOVA with Dunnett's post hoc analysis using GraphPad Prism 7.0 (GraphPad Software, Inc.).



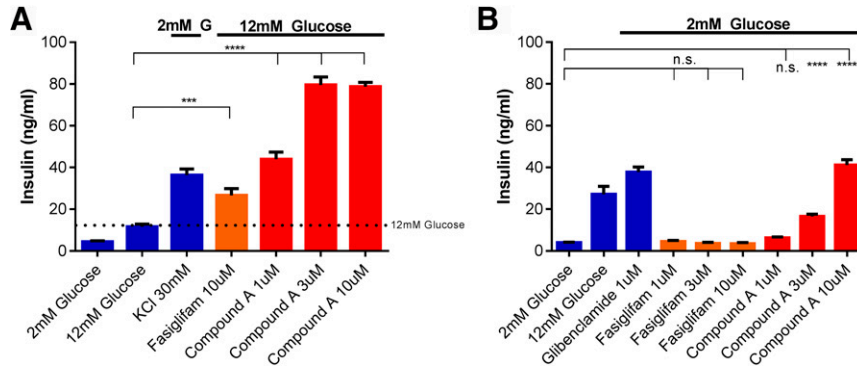


**Fig. 2.** Compound A is fully efficacious at potentiating GSIS in human islets. All donors tested were responsive to 12 mM glucose and non glucose-dependent insulin secretagogues, KCl or glibenclamide. (A) In the presence of 12 mM glucose, Compound A significantly potentiated insulin secretion compared with islets treated with glucose alone. The potentiation observed with fasiglifam was  $22.4\% \pm 6\%$  ( $P < 0.0001$ ) of the potentiation induced by Compound A. (B) In the presence of low glucose (2 mM), fasiglifam was not able to potentiate GSIS. Stimulation with Compound A led to significant potentiation of insulin secretion but at higher concentrations than in the presence of high glucose. Data are represented as averages  $\pm$  S.E.M. from three different islets. Donors are different between graphs (A and B). Statistical significance was determined by one-way ANOVA with Dunnett's post hoc analysis using GraphPad Prism 7.0 (GraphPad Software, Inc.).

and BRET sensors provide a straightforward approach to directly assess G protein activation, independently of downstream effectors and potential cross regulation between pathways. Compared with the IP1 assay, we obtained similar results with the  $G\alpha q$  and  $G\alpha 11$  sensors (Fig. 3A; Supplemental Fig. 2A). Compound A was a full agonist at the  $G\alpha q$  and  $G\alpha 11$  pathways with similar efficacy as  $\alpha$ -linolenic acid, an endogenous GPR40 agonist, as well as AM-1638, and fasiglifam was a partial agonist with about 40% efficacy ( $P < 0.0001$ ) (Fig. 3A; Table 1). However, in contrast to the IP1 assay, fasiglifam was less potent than Compound A and AM-1638 at recruiting  $G\alpha q$  (Table 1), suggesting fasiglifam might trigger the activation of other pathways leading to IP1 accumulation. Additionally, at both the  $G\alpha q$  and  $G\alpha 11$  pathways, Compound A- and AM-1638-induced responses, but not that induced by fasiglifam, appeared highly cooperative (Hill slope  $> 1$ ) (Table 1).

We then measured the ability of Compound A to activate the  $Gai/o$  pathway in hGPR40 expressing cells using  $Gai2$  (Fig. 3B),  $G\alpha oB$ , and  $G\alpha z$  sensors (Table 1). Both Compound A and AM-1638 were full agonists at the  $Gai/o$  pathway (Fig. 3B; Table 1) compared to  $\alpha$ -linolenic acid, with Compound A being slightly more potent (Table 1). Interestingly, fasiglifam displayed intra- $Gai/o$  family bias by promoting partial activation

of  $Gai2$  (~50% efficacy compared with Compound A and AM-1638), while being completely inactive on  $G\alpha oB$  and  $G\alpha z$  (Fig. 3B; Table 1).

Compared to Compound A and AM-1638, fasiglifam was more potent at recruiting  $Gai2$  than  $G\alpha q/11$  (Fig. 3, A and B; Table 1). Using the Black-Leff operational model and  $\alpha$ -linolenic acid as a reference compound, we evaluated that fasiglifam was biased toward  $Gai2$  versus  $G\alpha q$  (bias factor = 5.86 compared to 0.19 for both Compound A and AM-1638), while Compound A and AM-1638 were slightly biased toward  $G\alpha q$  versus  $Gai2$  (bias factor = 5.2 compared to 0.17 for fasiglifam). These data could explain why fasiglifam was more potent than Compound A and AM-1638 at the IP1 pathway compared with the  $G\alpha q$  activation assay. It is, in fact, well known that  $Gai/o$  coupling can lead to IP production and calcium signaling (Rives et al., 2009). To confirm the involvement of the  $Gai/o$  pathway in fasiglifam-induced IP1 responses, we measured GPR40-mediated IP1 production following treatment with Compound A, AM-1638, and fasiglifam in the presence of PTX. PTX activity was first validated using the BRET  $G\alpha q$  and  $Gai2$  sensors. While PTX had no significant effect on  $G\alpha q$  activation (Supplemental Fig. 3A), it completely abolished  $Gai2$  coupling (Supplemental Fig. 3B).

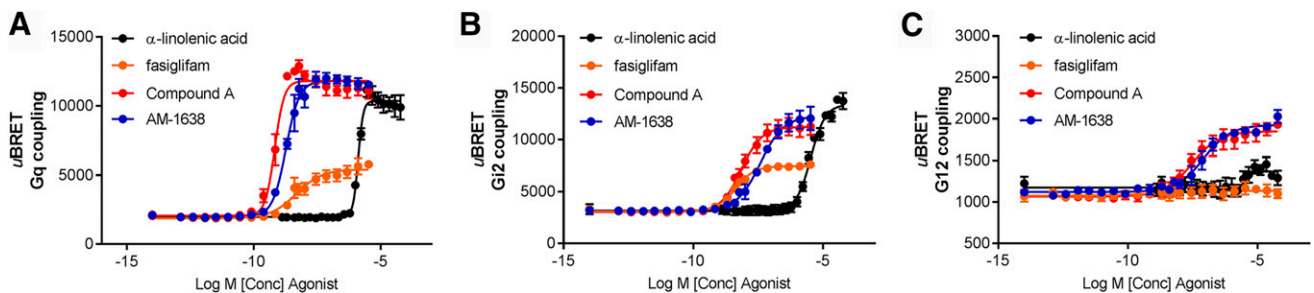


**Fig. 3.** Compound A is a full agonist at  $G\alpha q$  and  $Gai2$  and engages the  $G\alpha 12$  pathway. (A–C) BRET-based biosensor assays were used to directly monitor G protein activation following GPR40 agonist treatment. (A)  $G\alpha q$  sensor. Compound A and AM-1638 were full agonists at the  $G\alpha q$  pathway with similar efficacy as  $\alpha$ -linolenic acid. Fasiglifam was a partial agonist with about 40% efficacy compared with Compound A. (B)  $Gai2$  sensor. Compound A and AM-1638 were highly efficacious agonists at the  $Gai2$  pathway with  $82.5\% \pm 4.6\%$  and  $91.6\% \pm 4.5\%$  efficacy, respectively, compared with  $\alpha$ -linolenic acid. Fasiglifam was a partial agonist at  $Gai2$  with about 40% efficacy ( $43.5\% \pm 2.0\%$ ;  $P < 0.0001$ ) compared with Compound A. (C)  $G\alpha 12$  sensor. While fasiglifam was inactive at  $G\alpha 12$ , Compound A and AM-1638 induced activation of the  $G\alpha 12$  protein similarly to the ghrelin receptor (Supplemental Fig. 2B) (Sivertsen et al., 2011; Evron et al., 2014). Symbols represent the mean  $\pm$  S.E.M. from at least three independent experiments performed in duplicates.

TABLE 1

Potency ( $EC_{50}$ ) and efficacy relative to  $\alpha$ -linolenic acid ( $E_{max}$ , percentage of  $\alpha$ -linolenic acid  $\pm$  S.D.) of fasiglifam, Compound A, and AM-1638 at multiple G proteins using BRET-based sensors

G Protein and Parameters	Fasiglifam	Compound A	AM-1638
<b>Gq</b>			
$E_{max}$ (% $\alpha$ -linolenic acid)	40.9 $\pm$ 4.4 <sup>a</sup>	112.8 $\pm$ 5.6	115.2 $\pm$ 2.9
$EC_{50}$ (nM) (average $\pm$ S.D.)	8.3 $\pm$ 2.2 <sup>a</sup>	0.55 $\pm$ 0.03	1.9 $\pm$ 0.3
Hill Slope, average (95% CI)	0.9 (0.5–1.5)	2.3 (1.7–4.4)	1.6 (1.3–2.1)
<b>G11</b>			
$E_{max}$ (% $\alpha$ -linolenic acid)	35.8 $\pm$ 4.4 <sup>a</sup>	122.7 $\pm$ 10.0	111.9 $\pm$ 9.4
$EC_{50}$ (nM) (average $\pm$ S.D.)	10.1 $\pm$ 4.9 <sup>a</sup>	0.3 $\pm$ 0.3	1.1 $\pm$ 0.3
Hill Slope, average (95% CI)	0.5 (0.3–0.8)	2.8 (2.0–6.5)	2.5 (1.7– $\infty$ )
<b>G12</b>			
$E_{max}$ (% $\alpha$ -linolenic acid)	N.A. <sup>b</sup>	>300	>300
$EC_{50}$ (nM) (average $\pm$ S.D.)	N.A. <sup>b</sup>	28.7 $\pm$ 12.5	83.9 $\pm$ 26.5
Hill Slope, average (95% CI)	N.A. <sup>b</sup>	0.8 (0.5–1.3)	0.8 (0.6–1.1)
<b>G13</b>			
$E_{max}$ (% $\alpha$ -linolenic acid)	N.A. <sup>b</sup>	>200	>200
$EC_{50}$ (nM) (average $\pm$ S.D.)	N.A. <sup>b</sup>	209 $\pm$ 105	154 $\pm$ 96
Hill Slope, average (95% CI)	N.A. <sup>b</sup>	1.0 (0.6–2.0)	1.0 (0.6–2.0)
<b>Gs</b>			
$E_{max}$ (% $\alpha$ -linolenic acid)	N.A. <sup>b</sup>	N.D.	N.D.
$EC_{50}$ (nM) (average $\pm$ S.D.)	N.A. <sup>b</sup>	N.D.	N.D.
Hill Slope, average (95% CI)	N.A. <sup>b</sup>	N.D.	N.D.
<b>Gi2</b>			
$E_{max}$ (% $\alpha$ -linolenic acid)	43.5 $\pm$ 2.0 <sup>a</sup>	82.5 $\pm$ 4.6	91.6 $\pm$ 4.5
$EC_{50}$ (nM) (average $\pm$ S.D.)	4.2 $\pm$ 1.0	7.2 $\pm$ 1.8	38.0 $\pm$ 9.3
Hill Slope, average (95% CI)	1.2 (0.9–1.6)	1.1 (0.8–1.5)	1.0 (0.8–1.2)
<b>GoB</b>			
$E_{max}$ (% $\alpha$ -linolenic acid)	N.A. <sup>b</sup>	72.9 $\pm$ 4.5	81.7 $\pm$ 5.9
$EC_{50}$ (nM) (average $\pm$ S.D.)	N.A. <sup>b</sup>	69.9 $\pm$ 84.1	277 $\pm$ 122
Hill Slope, average (95% CI)	N.A. <sup>b</sup>	0.7 (0.5–1.0)	0.6 (0.5–0.9)
<b>Gz</b>			
$E_{max}$ (% $\alpha$ -linolenic acid)	N.A. <sup>b</sup>	151.5 $\pm$ 10.0	148.4 $\pm$ 25.6
$EC_{50}$ (nM) (average $\pm$ S.D.)	N.A. <sup>b</sup>	11.5 $\pm$ 4.4	114 $\pm$ 58
Hill Slope, average (95% CI)	N.A. <sup>b</sup>	0.8 (0.7–0.9)	0.7 (0.6–0.9)

CI, confidence interval; N.A., not applicable; N.D., not determined.

<sup>a</sup>Significantly different from that of Compound A and AM-1638 ( $P < 0.05$ ).

<sup>b</sup> $EC_{50} > 50 \mu\text{M}$  and/or  $E_{max} < 10$ .

The efficacy of Compound A and AM-1638 at inducing IP1 production was not significantly affected by PTX treatment but the potency of both compounds was slightly reduced (3.5  $\pm$  0.4-fold and 2.4  $\pm$  0.1-fold, respectively) (Supplemental Fig. 3, C and D). However, fasiglifam-induced IP1 response was almost completely abolished by PTX treatment (Supplemental Fig. 3E), suggesting that in contrast to Compound A and AM-1638, fasiglifam-induced IP1 production was mostly driven by  $G\alpha i/o$  coupling.

We also profiled the activity of Compound A at the  $G\alpha 12/13$  pathway. Interestingly, while fasiglifam failed to recruit  $G\alpha 12$ , Compound A and AM-1638 strongly activated the  $G\alpha 12$  protein in hGPR40-expressing cells (Fig. 3C; Table 1). The magnitude of the  $G\alpha 12$  response following activation of hGPR40 by Compound A and AM-1638 was substantial and similar to that induced by ghrelin in cells expressing the ghrelin receptor (Supplemental Fig. 2B) (Sivertsen et al., 2011; Evron et al., 2014). Interestingly,  $\alpha$ -linolenic acid only very weakly activated the pathway, suggesting that the ability to activate  $G\alpha 12$  is a unique property of the synthetic full agonists AM-1638 and Compound A. We obtained similar results at  $G\alpha 13$  (Supplemental Fig. 2C). Although the  $G\alpha 12/G13$ -mediated signaling pathway is poorly understood, it has been linked to PKD activation as well as actin

remodeling (Yuan et al., 2001; Siehler, 2007), which are well known to contribute to the release of vesicles.

**Compound A Only Weakly Triggers Gas Activation/cAMP Production.** As mentioned previously, it has been shown that in addition to the  $G\alpha q/IP1$ /calcium pathway, some GPR40 agonists could induce coupling to other pathways (Schröder et al., 2011; Mancini and Poitout, 2013; Hauge et al., 2014, 2017; Mancini et al., 2015). More specifically, it has been shown that allosteric full agonists such as AM-1638, but not partial agonists, induced coupling to the  $G\alpha s/cAMP$  pathway and that only agonists at both  $G\alpha q$  and  $G\alpha s$  could trigger maximal efficacy in relevant preclinical models, such as GLP-1 secretion in mice (Luo et al., 2012; Hauge et al., 2014). To assess the ability of Compound A to induce signaling through the  $G\alpha s/cAMP$  pathway, we also used a BRET-based  $G\alpha s$  sensor (Fig. 4A). In cells transfected with the GLP-1 receptor, a well-known  $G\alpha s$ -coupled receptor, GLP-1[7–36] induced a strong  $G\alpha s$  response, confirming the functionality of the  $G\alpha s$  biosensor. However, in hGPR40-transfected cells, only a very weak response could be measured after stimulation with either Compound A or  $\alpha$ -linolenic acid, about 10%–20% of the GLP-1 response. Fasiglifam was inactive (Fig. 4A). Surprisingly, AM-1638 also only weakly induced  $G\alpha s$  activation (Fig. 4A).

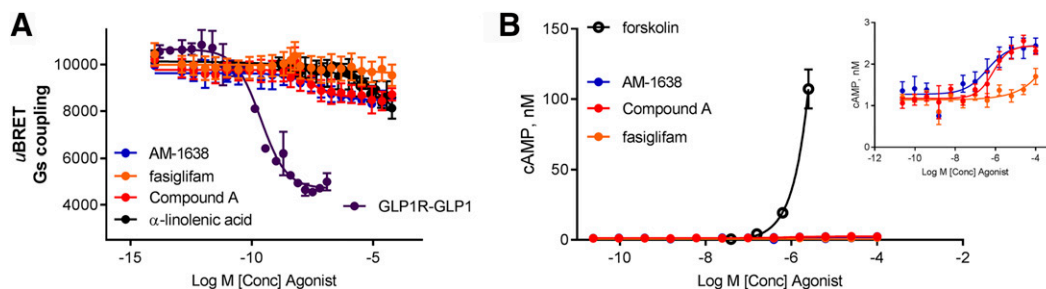


**Fig. 4.** Compound A and AM-1638 only weakly activate the  $G\alpha_s$ /cAMP pathway. (A) BRET-based  $G\alpha_s$  biosensor was used to directly monitor  $G\alpha_s$  protein activation following GPR40 agonist treatment. In cells transfected with the GLP-1 receptor, a well-known  $G\alpha_s$ -coupled receptor, GLP-1[7–36] induced a strong  $G\alpha_s$  response. In hGPR40-transfected cells, Compound A, AM-1638, and  $\alpha$ -linolenic acid only induced a very weak response and fasiglifam was inactive. (B) In hGPR40-expressing cells, fasiglifam was inactive at inducing increases in cAMP production and Compound A and AM-1638 only weakly activated the cAMP pathway compared with the forskolin control performed in the same cells. Data presented are representative of three independent experiments performed in quadruplicate for each compound. Data are represented as averages  $\pm$  S.D.

To confirm those findings, we also measured cAMP accumulation in the hGPR40 stable CHO-K1 cell line mentioned previously. As previously described (Hauge et al., 2014), fasiglifam was inactive and did not induce any significant increases in cAMP accumulation. Interestingly, although Compound A and AM-1638 induced some cAMP accumulation, the magnitude of the cAMP response was very weak compared with the forskolin control performed in the same cells (Fig. 4B).

**Compound A Is an Allosteric Full Agonist.** Three distinct binding sites have been described for GPR40, one that binds endogenous fatty acids such as  $\alpha$ -linolenic acid, one that binds partial agonists such as fasiglifam, and one that binds allosteric full agonists, such as AM-1638 and the recently reported AP8 (Lin et al., 2012; Defossa and Wagner, 2014; Hauge et al., 2014; Srivastava et al., 2014; Lu et al., 2017). The resolution of the crystal structure of hGPR40 in complex with both a partial agonist and the full agonist AP8 recently identified the allosteric full agonists' binding site as a lipid-facing pocket outside the transmembrane helical bundle (Lu et al., 2017), between TM4 and TM5.

To assess the orthosteric or allosteric nature of Compound A, we analyzed the functional cooperativity between  $\alpha$ -linolenic acid and Compound A using BRET-based  $G\alpha_q$  (Fig. 5A) and  $G\alpha_{i2}$  sensors (Fig. 5B) compared with that of fasiglifam and AM-1638. All three compounds could potentiate an  $EC_{20}$  of  $\alpha$ -linolenic acid at inducing  $G\alpha_q$  and  $G\alpha_{i2}$  coupling. The

relative potencies and efficacies of Compound A, AM-1638, and fasiglifam in (PAM) mode (Fig. 5) were consistent with those previously observed in agonist mode (Fig. 3). Compound A ( $0.17 \pm 0.04$  and  $2.0 \pm 0.4$  nM at  $G\alpha_q$  and  $G\alpha_{i2}$ , respectively) was slightly more potent than AM-1638 ( $0.6 \pm 0.3$  and  $5.0 \pm 1.5$  nM at  $G\alpha_q$  and  $G\alpha_{i2}$ , respectively) at potentiating  $\alpha$ -linolenic acid-induced  $G\alpha_q$  and  $G\alpha_{i2}$  coupling. Moreover, compared with Compound A and AM-1638, fasiglifam only induced a partial potentiation of  $\alpha$ -linolenic acid responses ( $60\% \pm 6\%$  and  $53\% \pm 3\%$  at  $G\alpha_q$  and  $G\alpha_{i2}$ , respectively) (Fig. 5). These data confirm the allosteric nature of Compound A, potentiating  $\alpha$ -linolenic acid-induced responses.

We then used a computational approach to assess whether Compound A could bind to the same binding site as other reported allosteric full agonists. Compound A was docked in the lipid-facing pocket identified by Lu et al. (2017) between TM4 and TM5. The best docking pose of Compound A revealed a similar binding mode as AP8 (Fig. 6A). Among the interactions between Compound A and the protein, the carboxylate group anchored the compound between TM4 and TM5 via a complex H-bond network with Ser123 and Tyr44, and probably with Tyr114 from intracellular loop 2, folded in an alpha helix in the presence of the full agonists (Fig. 6B). The 5-fluoro-2-methoxy phenyl ring formed a CH: $\pi$  interaction with the side chain of Pro194. The rest of Compound A made numerous Van der Waals contacts with the hydrophobic residues forming the binding groove (Ala98, Ala99, Ala102, Val126, Ile130,

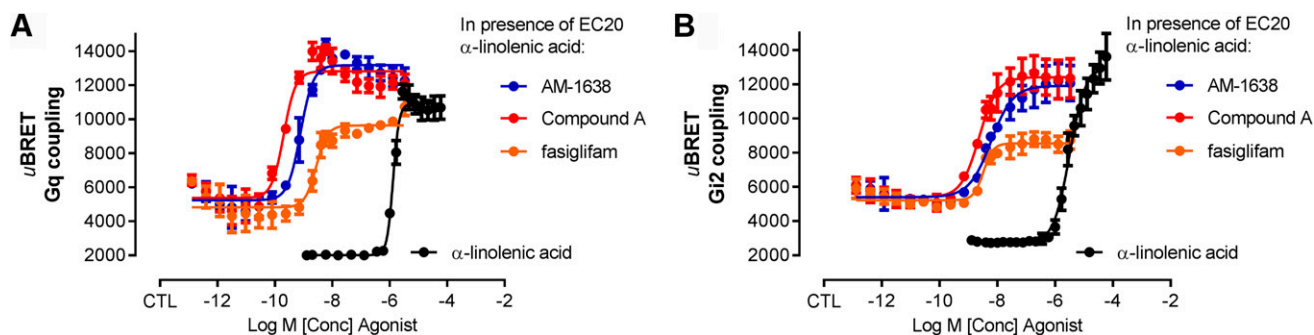


**Fig. 5.** Compound A, AM-1638, and fasiglifam potentiate  $\alpha$ -linolenic acid-induced coupling to  $G\alpha_q$  and  $G\alpha_{i2}$ . (A and B) BRET-based biosensor assays were used to directly monitor G protein activation following GPR40 agonist treatment. (A)  $G\alpha_q$  sensor. Compound A, AM-1638, and fasiglifam potentiated an  $EC_{20}$  of  $\alpha$ -linolenic acid at inducing  $G\alpha_q$  coupling to hGPR40. (B)  $G\alpha_{i2}$  sensor. Compound A, AM-1638, and fasiglifam potentiated an  $EC_{20}$  of  $\alpha$ -linolenic acid at inducing  $G\alpha_{i2}$  coupling to hGPR40. For each compound, data from two independent experiments performed in duplicates were combined and symbols presented are the mean  $\pm$  S.E.M.

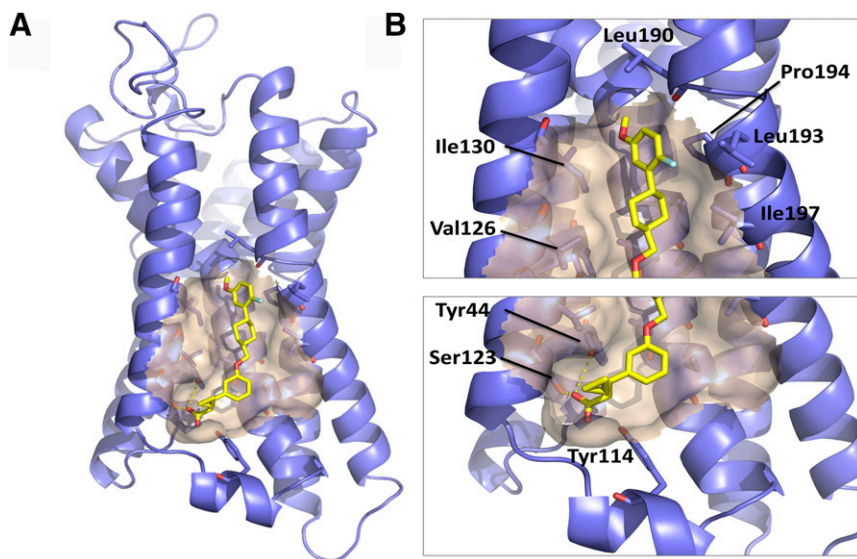


**Fig. 6.** Docking of Compound A in an allosteric pocket. (A) Docking of Compound A in the lipid-facing pocket between TM4 and TM5 identified by Lu et al. (2017) as the allosteric full agonists' binding site. (B) Ligand: receptor interactions between Compound A and hGPR40 predicted from the molecular docking of Compound A into in the lipid-facing pocket identified by Lu et al. (2017) between TM4 and TM5.

Leu193, and Ile197) (Fig. 6B). While it is clear that multiple ligand:protein interactions contribute to the potency of Compound A, the physicochemical properties of the compound suggest it could also make numerous contacts with surrounding membrane lipids (missing in the X-ray structure).

Furthermore, we also performed radioligand binding experiments using both [ $^3\text{H}$ ]-Compound A and [ $^3\text{H}$ ]-AM-1638, providing additional evidence that Compound A could bind to the same site as AM-1638. Competition binding experiments showed that Compound A, as well as AM-1638, completely displaced the binding of both [ $^3\text{H}$ ]-Compound A (Supplemental Fig. 4A) and [ $^3\text{H}$ ]-AM-1638 (Supplemental Fig. 4B). Data were fitted quite well by a one-site competition binding model (Supplemental Table 1), providing additional evidence that both compounds bind to an identical unique binding site. Additionally, fasiglifam had a positive cooperative effect on the binding of [ $^3\text{H}$ ]-Compound A (Supplemental Fig. 4A). The effects observed with fasiglifam are similar to those previously reported in the literature (Yabuki et al., 2013; Lu et al., 2017; Plummer et al., 2017) and are consistent with the allosteric nature of this compound.

## Discussion

GPR40 is a clinically validated molecular target for the treatment of diabetes. Although the partial agonist fasiglifam (TAK-875) showed efficacy in phase III clinical trials, its efficacy did not significantly differentiate from glimepiride and attention has shifted toward the development of full agonists that exhibit superior efficacy in preclinical models (Schröder et al., 2011; Luo et al., 2012; Hauge et al., 2014, 2017; Mancini et al., 2015). In the present study, we described the pharmacology of Compound A, a newly identified GPR40 allosteric full agonist at the  $G\alpha_q$ /IP1/calcium pathway fully efficacious at enhancing GSIS in human islets. We compared Compound A-induced GPR40 activity at a panel of G proteins and to that of both fasiglifam and AM-1638, another allosteric full agonist previously reported to be highly efficacious in preclinical models (Luo et al., 2012; Hauge et al., 2014).

In human islets, in the presence of high glucose, Compound A was highly efficacious at potentiating insulin secretion and

data were consistent with those reported for AM-1638 (Luo et al., 2012). Despite 40%–50% efficacy compared to Compound A and AM-1638 at the  $G\alpha_q$ /IP1/calcium pathway, in human islets and in presence of high glucose, fasiglifam efficacy was only about 22.4% of that of Compound A at potentiating insulin secretion. Moreover, Compound A, but not fasiglifam, could potentiate insulin secretion in low glucose conditions. These data suggest that the pharmacology of GPR40 is complex and that the activation of additional pathways might be responsible for the superior efficacy of Compound A in human islets.

Previous studies have suggested that activation of alternative pathways in addition to the  $G\alpha_q$ /calcium pathway was required for maximal efficacy in preclinical models (Lin et al., 2012; Defossa and Wagner, 2014; Hauge et al., 2014). Thus, only allosteric full agonists, such as AM-1638, which in

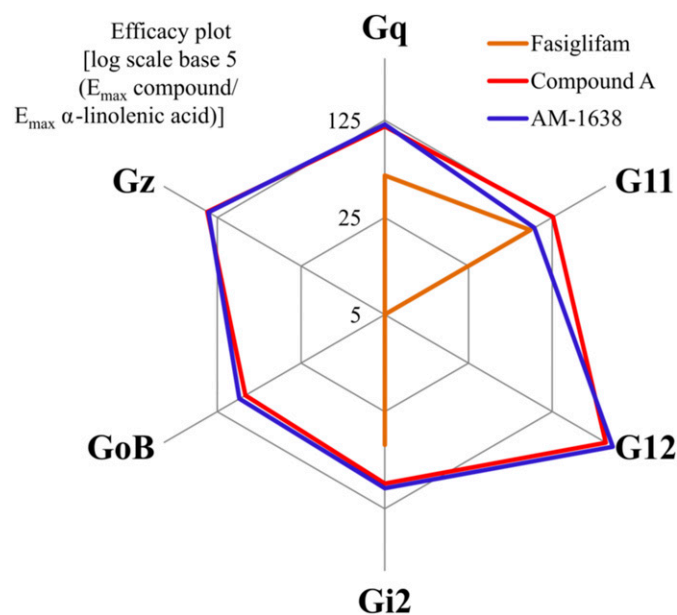


**Fig. 7.** Efficacy plot of Compound A, AM-1638, and fasiglifam at multiple G proteins compared to  $\alpha$ -linolenic acid: [ $\log$  scale base 5 ( $E_{\max}$  compound/ $E_{\max}$   $\alpha$ -linolenic acid)].



addition to the  $G\alpha q$ /calcium pathway were shown to induce cAMP production, could trigger maximal efficacy in preclinical models, such as GLP-1 secretion in mice (Luo et al., 2012; Hauge et al., 2014, 2017). Interestingly, even though Compound A binds to the same site as AM-1638 (Fig. 6; Supplemental Fig. 4), it showed no to very little efficacy at the  $G\alpha s$ /cAMP pathway. The magnitude of the cAMP response produced after stimulation with Compound A was very low and hGPR40 only very weakly coupled to  $G\alpha s$  after stimulation with Compound A (Fig. 4). Surprisingly, AM-1638 also only weakly induced  $G\alpha s$  activation and it is noteworthy that the magnitude of cAMP accumulation observed was similar to that previously reported (Hauge et al., 2014). Thus, although we cannot exclude the possibility that weak GPR40-mediated cAMP accumulation is enough to potentiate GLP-1 secretion or that mouse GPR40 coupling properties might significantly differ from hGPR40, our data suggest that hGPR40 does not efficiently couple to the  $G\alpha s$ /cAMP pathway and that pathways other than  $G\alpha s$  might be involved in GPR40 agonists in vivo efficacy. Moreover, our findings suggest that cAMP production measured in vitro may originate from other non- $G\alpha s$ -mediated couplings. It has indeed been shown that some adenylyl cyclase isoforms are calcium sensitive (Halls and Cooper, 2011), raising the possibility that the weak cAMP responses observed after GPR40 stimulation could come from cross regulation between pathways.

We, therefore, assessed the ability of our compound to induce the activation of other G proteins. Figure 7 shows an efficacy plot representing the relative efficacy of Compound A and AM-1638, as well as fasiglifam, relative to  $\alpha$ -linolenic acid at multiple G proteins. The graph highlights the ability of Compound A and AM-1638 to activate the  $G\alpha q/11$  and  $G\alpha i/o$  protein families, while fasiglifam was only a partial agonist at some of those pathways. The poor efficacy of fasiglifam is consistent with recent crystallography studies, showing that in complex with fasiglifam the intracellular portion of the receptors was in an inactive-like state (Srivastava et al., 2014; Lu et al., 2017). Moreover, in contrast to fasiglifam, at both  $G\alpha q$  and  $G\alpha 11$ , Compound A- and AM-1638-induced responses appeared highly cooperative (Hill slope  $> 1$ ) (Table 1). Since the binding data (Fig. 6; Supplemental Fig. 4; Supplemental Table 1) suggest the existence of only one binding site for these compounds, it is likely that Compound A and AM-1638 stabilize a unique conformation of the receptor, distinct from that stabilized by fasiglifam, and that this conformation is further stabilized by  $G\alpha q$ , but not other G proteins. It is indeed now well known that downstream effectors such as G proteins can allosterically modulate the receptor and stabilize active or inactive conformations (Rasmussen et al., 2011).

Although activation of the  $G\alpha q/IP1/Ca^{2+}$  pathway was shown to lead to insulin secretion and  $G\alpha i/o$  coupling is known to potentiate  $G\alpha q$ -mediated IP1 and calcium responses (Rives et al., 2009), the activation of  $G\alpha i/o$ -coupled receptors is usually associated with a decrease in GSIS, through the inhibition of adenylyl cyclases (Fridlyand and Philipson, 2016). In contrast to Compound A and AM-1638, fasiglifam appeared slightly biased toward  $G\alpha i2$  versus  $G\alpha q$  and fasiglifam-induced IP1 production was more sensitive to PTX treatment than that of Compound A and AM-1638. The extent to which these differences contribute to differences in efficacy and/or safety is not clear but it could explain the weak

efficacy of fasiglifam at potentiating GSIS ( $<25\%$ ) despite 40%–50% efficacy compared to Compound A and AM-1638 at the  $G\alpha q/IP1$  pathway.

Compound A and AM-1638 also induced hGPR40 coupling to  $G\alpha 12$  (Fig. 3C), while fasiglifam was inactive and  $\alpha$ -linolenic acid only weakly activated the pathway. Although other agonists should be evaluated in this assay, these data suggest that the ability to activate  $G\alpha 12$  is a unique property of synthetic allosteric full agonists. The role of the  $G\alpha 12/13$  pathway in insulin and incretin secretion is poorly understood but it has been linked to PKD activation as well as actin remodeling, well known to contribute to vesicle release (Siehler, 2007; Ferdaoussi et al., 2012; Kalwat and Thurmond, 2013; Arous and Halban, 2015). Insulin secretion in response to glucose is biphasic, with a rapid and transient first phase followed by a slower but prolonged second phase. It is believed that first-phase insulin secretion corresponds to the exocytosis of a readily releasable pool of insulin granules predocked at the plasma membrane, whereas the second phase relies on the mobilization of an intracellular granule pool to the plasma membrane via a process that requires cytoskeletal remodeling. PKD activation has also been linked to the second phase of insulin release (Ferdaoussi et al., 2012; Kalwat and Thurmond., 2013).

The  $G\alpha_{12}/G_{13}$  proteins activate the monomeric GTPases RhoA. RhoA effectors include Rho kinase, which leads to Jun kinase activation and the induction of actin stress fiber formation (Siehler, 2007). The involvement of the cytoskeleton in secretion mechanisms was proposed almost 50 years ago, and although the precise mechanisms are not yet fully understood, it is now well accepted that actin regulates insulin granule trafficking and exocytosis (Arous and Halban, 2015). Constitutively active  $G\alpha 12/13$  was found to induce stress fiber formation and focal adhesion assembly in fibroblasts, similarly to activated  $G\alpha 12/13$ -linked lysophosphatidic acid receptors and constitutively active RhoA Q63L (Siehler, 2007). This suggests that  $G\alpha 12$  activation might play a critical role in secretion mechanisms, and our data raise the intriguing possibility that despite weak  $G\alpha s$  signaling, the ability of Compound A and AM-1638 to signal through the  $G\alpha_{12}$  pathway may contribute to the release of vesicles and be an important determinant of GPR40 agonist efficacy. It would be interesting to assess the efficacy of Compound A in mice at inducing GLP-1 secretion, as well as in type-2 diabetes human islets where actin remodeling has been shown to be altered (Arous and Halban, 2015). Although the role of  $G\alpha 12/13$  downstream of GPR40 in insulin and incretin secretion needs to be validated both ex vivo and in vivo, while Compound A was more potent at  $G\alpha q$  and  $G\alpha i2$  compared to  $G\alpha 12$  (Table 1), in human islets, it is noteworthy that Compound A showed maximal efficacy only at concentrations greater than 1  $\mu M$  (Fig. 2).

Nevertheless, the superior efficacy of Compound A in human islets in low glucose conditions suggests that Compound A administration might lead to hypoglycemia and activation of  $G\alpha 12/13$  could be contraindicated to avoid insulin secretion in low glucose conditions. Moreover, in addition to its role in insulin secretion, PKD activation has been linked to NF- $\kappa B$  activation, the development of inflammation, and pancreatitis (Yuan and Pandol, 2016). Although GPR40 does not seem expressed in the exocrine pancreas, it would be interesting to assess whether Compound A could yield inflammatory responses after either acute or chronic treatment.

In conclusion, we have identified Compound A, a new GPR40 allosteric full agonist fully efficacious at enhancing GSIS in human islets. Compound A was a full agonist at  $G_{\alpha q}$ ,  $G_{\alpha i2}$ , and  $G_{\alpha 12}$ , with no to very weak efficacy at the  $G_{\alpha s}/cAMP$  pathway. Although more work is needed to validate the role of the GPR40-mediated  $G_{\alpha 12}$  pathway in secretion mechanisms, our data suggest that the pharmacology of GPR40 is complex and that engagement of multiple signaling pathways may be critical to achieve sufficient therapeutic efficacy.

#### Acknowledgments

The authors thank Dr. Alan Wickenden for helpful comments on the manuscript.

#### Authorship Contributions

*Participated in research design:* Rives, Rady, Zhao, Bakaj, Lee, Player, Pocai.

*Conducted experiments:* Rives, Rady, Swanson, Zhao, Qi, Bakaj, Mancini.

*Contributed new reagents or analytic tools:* Player.

*Performed data analysis:* Rives, Rady, Zhao, Arnoult, Bakaj, Mancini, Breton, Lee, Player, Pocai.

*Wrote or contributed to the writing of the manuscript:* Rives, Rady, Arnoult, Mancini, Breton, Player.

#### References

- Arous C and Halban PA (2015) The skeleton in the closet: actin cytoskeletal remodeling in  $\beta$ -cell function. *Am J Physiol Endocrinol Metab* **309**:E611–E620.
- Baggio LL and Drucker DJ (2007) Biology of incretins: GLP-1 and GIP. *Gastroenterology* **132**:2131–2157.
- Briscoe CP, Peat AJ, McKeown SC, Corbett DF, Goetz AS, Littleton TR, McCoy DC, Kenakin TP, Andrews JL, Ammala C, et al. (2006) Pharmacological regulation of insulin secretion in MIN6 cells through the fatty acid receptor GPR40: identification of agonist and antagonist small molecules. *Br J Pharmacol* **148**: 619–628.
- Briscoe CP, Tadayyon M, Andrews JL, Benson WG, Chambers JK, Eilert MM, Ellis C, Elshourbagy NA, Goetz AS, Minnick DT, et al. (2003) The orphan G protein-coupled receptor GPR40 is activated by medium and long chain fatty acids. *J Biol Chem* **278**:11303–11311.
- Burant CF, Viswanathan P, Marcinak J, Cao C, Vakilynejad M, Xie B, and Leifke E (2012) TAK-875 versus placebo or glimepiride in type 2 diabetes mellitus: a phase 2, randomised, double-blind, placebo-controlled trial. *Lancet* **379**:1403–1411.
- Cassutt KJ, Orsini MJ, Abouleiman M, Colone D, and Tang W (2007) Identifying nonselective hits from a homogeneous calcium assay screen. *J Biomol Screen* **12**: 285–287.
- Corbeil CR, Williams CI, and Labute P (2012) Variability in docking success rates due to dataset preparation. *J Comput Aided Mol Des* **26**:775–786.
- Costa-Neto CM, Parreiras-E-Silva LT, and Bouvier M (2016) A pluridimensional view of biased agonism. *Mol Pharmacol* **90**:587–595.
- Defossa E and Wagner M (2014) Recent developments in the discovery of FFA1 receptor agonists as novel oral treatment for type 2 diabetes mellitus. *Bioorg Med Chem Lett* **24**:2991–3000.
- Denis C, Saulière A, Galandrin S, Sénard JM, and Galés C (2012) Probing heterotrimeric G protein activation: applications to biased ligands. *Curr Pharm Des* **18**: 128–144.
- Edfalk S, Steneberg P, and Edlund H (2008) *Gpr40* is expressed in enteroendocrine cells and mediates free fatty acid stimulation of incretin secretion. *Diabetes* **57**: 2280–2287.
- Evron T, Peterson SM, Urs NM, Bai Y, Rochelle LK, Caron MG, and Barak LS (2014) G Protein and  $\beta$ -arrestin signaling bias at the ghrelin receptor. *J Biol Chem* **289**: 33442–33455.
- Ferdaoussi M, Bergeron V, Zarrouki B, Kolic J, Cantley J, Fielitz J, Olson EN, Prentki M, Biden T, MacDonald PE, et al. (2012) G protein-coupled receptor (GPR)40-dependent potentiation of insulin secretion in mouse islets is mediated by protein kinase D1. *Diabetologia* **55**:2682–2692.
- Fridlyand LE and Philipson LH (2016) Pancreatic beta cell G-protein coupled receptors and second messenger interactions: a systems biology computational analysis. *PLoS One* **11**:e0152869.
- Gorski JN, Pachanski MJ, Mane J, Plummer CW, Souza S, Thomas-Fowlkes BS, Ogawa AM, Weinglass AB, Di Salvo J, Cheewatrakoolpong B, et al. (2017) GPR40 reduces food intake and body weight through GLP-1. *Am J Physiol Endocrinol Metab* **313**:E37–E47.
- Halls ML and Cooper DM (2011) Regulation by  $Ca^{2+}$ -signaling pathways of adenylyl cyclases. *Cold Spring Harb Perspect Biol* **3**:a004143.
- Hardy S, St-Onge GG, Joly E, Langelier Y, and Prentki M (2005) Oleate promotes the proliferation of breast cancer cells via the G protein-coupled receptor GPR40. *J Biol Chem* **280**:13285–13291.
- Hauge M, Ekberg JP, Engelstoft MS, Timshel P, Madsen AN, and Schwartz TW (2017) Gq and Gs signaling acting in synergy to control GLP-1 secretion. *Mol Cell Endocrinol* **449**:64–73.
- Hauge M, Vestmar MA, Husted AS, Ekberg JP, Wright MJ, Di Salvo J, Weinglass AB, Engelstoft MS, Madsen AN, Lückmann M, et al. (2014) GPR40 (FFAR1)-combined Gs and Gq signaling in vitro is associated with robust incretin secretagogue action ex vivo and in vivo. *Mol Metab* **4**:3–14.
- Hedington MS and Davis SN (2014) Discontinued in 2013: diabetic drugs. *Expert Opin Investig Drugs* **23**:1703–1711.
- Holst JJ (2007) The physiology of glucagon-like peptide 1. *Physiol Rev* **87**:1409–1439.
- Itoh Y, Kawamata Y, Harada M, Kobayashi M, Fujii R, Fukusumi S, Ogi K, Hosoya M, Tanaka Y, Uejima H, et al. (2003) Free fatty acids regulate insulin secretion from pancreatic  $\beta$  cells through GPR40. *Nature* **422**:173–176.
- Jin J, Mao Y, Thomas D, Kim S, Daniel JL, and Kunapuli SP (2009) RhoA downstream of  $G_{\alpha q}$  and  $G_{12/13}$  pathways regulates protease-activated receptor-mediated dense granule release in platelets. *Biochem Pharmacol* **77**:835–844.
- Kaku K, Enya K, Nakaya R, Ohira T, and Matsuno R (2015) Efficacy and safety of fasiglifam (TAK-875), a G protein-coupled receptor 40 agonist, in Japanese patients with type 2 diabetes inadequately controlled by diet and exercise: a randomized, double-blind, placebo-controlled, phase III trial. *Diabetes Obes Metab* **17**: 675–681.
- Kalwat MA and Thurmond DC (2013) Signaling mechanisms of glucose-induced F-actin remodeling in pancreatic islet  $\beta$  cells. *Exp Mol Med* **45**:e37.
- Kenakin T and Christopoulos A (2013) Signalling bias in new drug discovery: detection, quantification and therapeutic impact. *Nat Rev Drug Discov* **12**: 205–216.
- Kenakin T, Watson C, Muniz-Medina V, Christopoulos A, and Novick S (2012) A simple method for quantifying functional selectivity and agonist bias. *ACS Chem Neurosci* **3**:193–203.
- Latour MG, Alquier T, Oseid E, Tremblay C, Jetton TL, Luo J, Lin DC, and Poutou V (2007) GPR40 is necessary but not sufficient for fatty acid stimulation of insulin secretion in vivo. *Diabetes* **56**:1087–1094.
- Leifke E, Naik H, Wu J, Viswanathan P, Demanno D, Kipnes M, and Vakilynejad M (2012) A multiple-ascending-dose study to evaluate safety, pharmacokinetics, and pharmacodynamics of a novel GPR40 agonist, TAK-875, in subjects with type 2 diabetes. *Clin Pharmacol Ther* **92**:29–39.
- Li Z, Qiu Q, Geng X, Yang J, Huang W, and Qian H (2016) Free fatty acid receptor agonists for the treatment of type 2 diabetes: drugs in preclinical to phase II clinical development. *Expert Opin Investig Drugs* **25**:871–890.
- Lin DC, Guo Q, Luo J, Zhang J, Nguyen K, Chen M, Tran T, Dransfield PJ, Brown SP, Houze J, et al. (2012) Identification and pharmacological characterization of multiple allosteric binding sites on the free fatty acid 1 receptor. *Mol Pharmacol* **82**:843–859.
- Lu J, Byrne N, Wang J, Bricogne G, Brown FK, Chobanian HR, Colletti SL, Di Salvo J, Thomas-Fowlkes B, Guo Y, et al. (2017). Structural basis for the cooperative allosteric activation of the free fatty acid receptor GPR40. *Nat Struct Mol Biol* **24**: 570–577.
- Luo J, Swaminath G, Brown SP, Zhang J, Guo Q, Chen M, Nguyen K, Tran T, Miao L, Dransfield PJ, et al. (2012) A potent class of GPR40 full agonists engages the enteroinular axis to promote glucose control in rodents. *PLoS One* **7**:e46300.
- Mancini AD, Bertrand G, Vivot K, Carpentier É, Tremblay C, Ghislain J, Bouvier M, and Poutou V (2015)  $\beta$ -Arrestin recruitment and biased agonism at free fatty acid receptor 1. *J Biol Chem* **290**:21131–21140.
- Mancini AD and Poutou V (2013) The fatty acid receptor FFA1/GPR40 a decade later: how much do we know? *Trends Endocrinol Metab* **24**:398–407.
- Namkung Y, Le Gouill C, Lukashova V, Kobayashi H, Hogue M, Khoury E, Song M, Bouvier M, and Laporte SA (2016) Monitoring G protein-coupled receptor and  $\beta$ -arrestin trafficking in live cells using enhanced bystander BRET. *Nat Commun* **7**:12178.
- Otieno MA, Snoeys J, Lam W, Ghosh A, Player MR, Pocai A, Salter R, Simic D, Skaggs H, Singh B, et al. (2017). Fasiglifam (TAK-875): mechanistic investigation and retrospective identification of hazards for drug induced liver injury. *Toxicol Sci* DOI: 10.1093/toxsci/kfx040 [published ahead of print].
- Plummer CW, Clements MJ, Chen H, Rajagopalan M, Josien H, Hagmann WK, Miller M, Trujillo ME, Kirkland M, Kosinski D, et al. (2017) Design and synthesis of novel, selective GPR40 Agonists. *ACS Med Chem Lett* **8**:221–226.
- Pocai A (2012) Unraveling oxyntomodulin, GLP1's enigmatic brother. *J Endocrinol* **215**:335–346.
- Rankovic Z, Brust TF, and Bohn LM (2016) Biased agonism: an emerging paradigm in GPCR drug discovery. *Bioorg Med Chem Lett* **26**:241–250.
- Rasmussen SG, DeVree BT, Zou Y, Kruse AC, Chung KY, Kobilka TS, Thian FS, Chae PS, Pardon E, Calinski D, et al. (2011) Crystal structure of the  $\beta_2$  adrenergic receptor-Gs protein complex. *Nature* **477**:549–555.
- Rives ML, Vol C, Fukazawa Y, Tinel N, Trinquet E, Ayoub MA, Shigemoto R, Pin JP, and Prézeau L (2009) Crosstalk between GABA<sub>A</sub> and mGlu1 receptors reveals new insight into GPCR signal integration. *EMBO J* **28**:2195–2208.
- Salahpour A, Espinoza S, Masri B, Lam V, Barak LS, and Gainetdinov RR (2012) BRET biosensors to study GPCR biology, pharmacology, and signal transduction. *Front Endocrinol (Lausanne)* **3**:105.
- Schröder R, Schmidt J, Blättermann S, Peters L, Janssen N, Grundmann M, Seemann W, Kaufel D, Merten N, Drecke C, et al. (2011) Applying label-free dynamic mass redistribution technology to frame signaling of G protein-coupled receptors noninvasively in living cells. *Nat Protoc* **6**:1748–1760.
- Shapiro H, Shachar S, Sekler I, Hershinkel M, and Walker MD (2005) Role of GPR40 in fatty acid action on the beta cell line INS-1E. *Biochem Biophys Res Commun* **335**:97–104.
- Siehler S (2007)  $G_{12/13}$ -dependent signaling of G-protein-coupled receptors: disease context and impact on drug discovery. *Expert Opin Drug Discov* **2**: 1591–1604.
- Sivertsen B, Lang M, Frimurer TM, Holliday ND, Bach A, Els S, Engelstoft MS, Petersen PS, Madsen AN, Schwartz TW, et al. (2011) Unique interaction pattern for a functionally biased ghrelin receptor agonist. *J Biol Chem* **286**: 20845–20860.

- Srivastava A, Yano J, Hirozane Y, Kefala G, Gruswitz F, Snell G, Lane W, Ivetac A, Aertgeerts K, Nguyen J, et al. (2014) High-resolution structure of the human GPR40 receptor bound to allosteric agonist TAK-875. *Nature* **513**:124–127.
- Stoddart LA, Smith NJ, and Milligan G (2008) International Union of Pharmacology. LXXI. Free fatty acid receptors FFA1, -2, and -3: pharmacology and pathophysiological functions. *Pharmacol Rev* **60**:405–417.
- Tomita T, Masuzaki H, Noguchi M, Iwakura H, Fujikura J, Tanaka T, Ebihara K, Kawamura J, Komoto I, Kawaguchi Y, et al. (2005) GPR40 gene expression in human pancreas and insulinoma. *Biochem Biophys Res Commun* **338**: 1788–1790.
- Yabuki C, Komatsu H, Tsujihata Y, Maeda R, Ito R, Matsuda-Nagasumi K, Sakuma K, Miyawaki K, Kikuchi N, Takeuchi K, et al. (2013) A novel antidiabetic drug, fasiglifam/TAK-875, acts as an ago-allosteric modulator of FFAR1. *PLoS One* **8**: e76280.
- Yonezawa T, Katoh K, and Obara Y (2004) Existence of GPR40 functioning in a human breast cancer cell line, MCF-7. *Biochem Biophys Res Commun* **314**: 805–809.
- Yuan J and Pandol SJ (2016) PKD signaling and pancreatitis. *J Gastroenterol* **51**: 651–659.
- Yuan J, Slice LW, and Rozengurt E (2001) Activation of protein kinase D by signaling through Rho and the  $\alpha$  subunit of the heterotrimeric G protein G<sub>13</sub>. *J Biol Chem* **276**:38619–38627.

---

**Address correspondence to:** Dr. Marie-Laure Rives, Molecular and Cellular Pharmacology, Janssen, Pharmaceutical companies of Johnson & Johnson, 3210 Merryfield Road, San Diego, CA 92121. E-mail: mrives1@its.jnj.com

---